4-Me-L-2,2,2, 4,7-Me_2-L-2,2,2, 4-Et-L-2,2,2, and 4-Me-L-2,3,2, respectively, in the presence and absence of Cu^{2+} at 25.0 ± 0.1 °C and μ = 0.10 M ($NaClO_4$), Figures 5S–8S, showing the results of Job's method of isomolar solutions of copper(II) and (4-Me-L-2,2,2), copper(II) and (4,7-Me-L-2,2,2), copper(II) and (4-Et-L-2,2,2), and copper(II) and (4-Me-L-2,3,2), respectively, at 25.0 ± 0.1 °C and μ = 0.10 M ($NaClO_4$), Figures 9S–11S, showing the electronic absorption spectra of copper(II) and (4-Me-L-2,2,2), copper(II) and (4-Et-L-2,2,2), and copper(II) and (4-Me-L-2,3,2) solutions, respectively, Figures 12S–15S, showing the degree of formation of copper (II)–(4,7-Me_2-L-2,2,2), copper(II)–(4-Me-L-2,3,2), copper(II)–(4-Et-L-2,2,2), and copper(II)–(4-Me-L-2,3,2) complexes, respectively, in 1:1 metal–ligand solution, Figures 16S–18S, showing the observed first-order rate constants (k_{obs}) as a function of $[Cu^{2+}]$ for the formation of $[Cu(4,7\text{-}Me_2\text{-}L\text{-}2,2,2)]^{2+}$, $[Cu(4\text{-}Me\text{-}L\text{-}2,2,2)]^{2+}$, and $[Cu(4\text{-}Et\text{-}L\text{-}2,2,2)]^{2+}$, respectively, at 25.0 ± 0.1 °C and μ = 0.1 M ($NaClO_4$), Figures 19S–21S, showing the resolution of the formation rate constants for copper(II) reacting with unprotonated and monoprotonated 4-Me-L-2,2,2, 4-Et-L-2,2,2, and 4,7-Me_2-L-2,2,2, respectively, at 25.0 ± 0.1 °C and μ = 0.10 M ($NaClO_4$), Figure 22S, showing the observed rate constants (k_{obs}) as a function of $[Cu^{2+}]$ for the formation of $[Cu(4\text{-}Me\text{-}L\text{-}2,3,2)]^{2+}$ at 25.0 ± 0.1 °C and μ = 0.10 M ($NaClO_4$), Figure 23S, showing the resolution of the formation rate constants for copper(II) reacting with unprotonated and monoprotonated 4-Me-L-2,3,2 at 25.0 ± 0.1 °C and μ = 0.10 M ($NaClO_4$), and Figure 24S, showing the resolution of the dissociation rate constants involving proton-independent and proton-dependent terms for $[Cu(4\text{-}Me\text{-}L\text{-}2,3,2)]^{2+}$ at 25.0 ± 0.1 °C and μ = 0.10 M ($NaClO_4$) (34 pages). Ordering information is given on any current masthead page.

Contribution from the Department of Chemistry,
The University, Southampton SO9 5NH, England

Chelating Ditelluroether Complexes of Palladium and Platinum: Synthesis and Multinuclear NMR Studies. Structure of Dibromo(*meso*-1,3-bis(phenyltelluro)propane)palladium(II), [Pd{*meso*-$PhTe(CH_2)_3TePh$}Br_2]

Tim Kemmitt, William Levason,* and Michael Webster

Received July 12, 1988

Palladium(II) and platinum(II) complexes of two chelating ditelluroether ligands $[M(L\text{-}L)X_2]$ (M = Pd or Pt, X = Cl, Br, or I, and L-L = $PhTe(CH_2)_3TePh$ or $MeTe(CH_2)_3TeMe$) are described. The complexes have been characterized by analysis and IR, UV–visible and multinuclear NMR (^1H, $^{125}Te\{^1H\}$, $^{195}Pt\{^1H\}$) spectroscopy. The NMR studies show that two diastereoisomers of the ligand are present in solution in each complex, *meso* and *dl* invertomers, with the former having the higher abundance. The structure of [Pd{*meso*-$PhTe(CH_2)_3TePh$}Br_2] has been determined by X-ray diffraction. Crystals belong to the triclinic crystal system, space group $P\bar{1}$, with a = 8.968 (1) Å, b = 10.978 (1) Å, c = 11.070 (2) Å, α = 108.16 (1)°, β = 113.15 (1)°, γ = 98.95 (1)°, and Z = 2. The structure was refined to an R value of 0.023 from 2545 reflections ($F > 3\sigma(F)$). The trends in the ^{125}Te and ^{195}Pt NMR chemical shifts and $^1J(^{195}Pt\text{–}^{125}Te)$ coupling constants are reported and discussed and are compared with data on the corresponding diselenoether complexes. Close parallels exist between ^{125}Te and ^{77}Se chemical shifts in comparable complexes. Attempts to halogen oxidize the complexes to the M(IV) state have failed.

Introduction

The coordination chemistry of organotellurium ligands is mainly limited to complexes of RTe^-, R_2Te, and R_2Te_2.[1] All attempts to prepare 1,2-di-R-telluroethanes have failed,[2,3] but we have recently reported[3] that 1,3-di-R-telluropropanes, $RTe(CH_2)_3TeR$ (R = Me or Ph), can be made in high yield from RTeLi and $Cl(CH_2)_3Cl$ at low temperatures. Here we report the synthesis and properties of palladium and platinum complexes of these two ligands and their ^1H, $^{125}Te\{^1H\}$, and $^{195}Pt\{^1H\}$ NMR spectra. The work is an extension of our previous studies of diselenoether complexes[4,5] with which detailed comparisons are drawn.

Results and Discussion

The reaction of $MeTe(CH_2)_3TeMe$ or $PhTe(CH_2)_3TePh$ with the appropriate $[M(MeCN)_2X_2]$ (M = Pd or Pt, X = Cl, Br or I) in CH_2Cl_2 or MeCN gave $[M\{RTe(CH_2)_3TeR\}X_2]$ complexes (Table I). There is no evidence for the formation of $[M(RTe(CH_2)_3TeR)_2]^{2+}$ ions even with a large excess of ligand. The solid complexes are air-stable in contrast to the air-sensitivity of the free ligands[3] and are poorly soluble in chlorocarbons and MeCN to give stable solutions. The complexes are more soluble in dimethyl sulfoxide (DMSO) and in *N*,*N*-dimethylformamide (DMF); however, decomposition is often apparent in DMSO over time. The physical data (Table I) are consistent with the formulation of all twelve complexes as cis planar materials, and this is confirmed by comparison with the data for the thio-[6] and selenoether[4] analogues, and by the X-ray study of [Pd{$PhTe(CH_2)_3TePh$}Br_2] (below). Chelating bidentate group 16 donor ligand complexes exist in two isomeric forms, containing *meso* and *dl* geometries (Figure 1), and these interconvert by pyramidal inversion at the heteroatoms.[7]

Structure of [Pd{$PhTe(CH_2)_3TePh$}Br_2]. The structure in the solid state consists of discrete molecules and is shown in Figure 2. The expected square-planar geometry around the Pd is found, and the principal feature of interest is the stereochemistry of the chelating ditellurium ligand. Inspection of the crystallographic literature[8] shows few examples of the monodentate Te ligands R_2Te and apparently no examples of chelating ditellurium ligands although one example of a PTe donor ligand is known.[9] The Pd–Te distances in the present compound (2.528, 2.525 Å) (Table II) may be compared with 2.606 (1) Å in *trans*-$Pd(SCN)_2(TeR_2)_2$ (R = $Me_3Si(CH_2)_2$)[10] and the Pd–Br distance (2.480 (1) Å) with 2.456 (1), 2.468 (1) Å in *cis*-$PdBr_2(C_6H_{12}S_3)$[11] and 2.431 (1) Å

(1) For a recent excellent review see: Gysling, H. J.; In *The Chemistry of Organic Selenium and Tellurium Compounds*; Patai, S.; Rappoport, Z., Eds.; Wiley: New York, 1986; vol. 1, pp 679–855.
(2) Pathirana, H. M. K. K.; McWhinnie, W. R. *J. Chem. Soc. Dalton Trans.* **1986**, 2003.
(3) Hope, E. G.; Kemmitt, T.; Levason, W. *Organometallics* **1987**, *6*, 206; **1988**, *7*, 78.
(4) Gulliver, D. J.; Hope, E. G.; Levason, W.; Murray, S. G.; Marshall, G. L. *J. Chem. Soc., Dalton Trans.* **1985**, 1265.
(5) Hope, E. G.; Levason, W.; Webster, M.; Murray, S. G. *J. Chem. Soc., Dalton Trans.* **1986**, 1003.
(6) Hartley, F. R.; Murray, S. G.; Levason, W.; Soutter, H. E.; McAuliffe, C. A. *Inorg. Chim. Acta* **1979**, *35*, 265.
(7) For a review see: Abel, E. W.; Orrell, K. G.; Bhargava, S. K. *Prog. Inorg. Chem.* **1984**, *32*, 1.
(8) Cambridge Structural Database, University Chemical Laboratory, Cambridge, England.
(9) Gysling, H. J.; Luss, H. R. *Organometallics* **1984**, *3*, 596.
(10) Gysling, H. J.; Luss, H. R.; Smith, D. L. *Inorg. Chem.* **1979**, *18*, 2696.

0020-1669/89/1328-0692$01.50/0 © 1989 American Chemical Society

Table I. Selected Physical Data

complex	color	$E_{max}/10^3$ cm^{-1} (ϵ_{mol}/dm^3 mol^{-1} cm^{-1})[a]	ν(M-X)/cm^{-1} [c]	% C[d]	% H[d]	$\delta(^1H)$/ppm[e] meso	$\delta(^1H)$/ppm[e] dl
[Pd{MeTe(CH$_2$)$_3$TeMe}Cl$_2$]	yellow	25.97 (3460)[b]	288 (br)	11.9 (12.2)	2.4 (2.5)	2.25	2.21
[Pd{MeTe(CH$_2$)$_3$TeMe}Br$_2$]	orange	25.13 (4380)[b]	230	10.1 (10.3)	2.0 (2.1)	2.28	2.21
[Pd{MeTe(CH$_2$)$_3$TeMe}I$_2$]	red	21.98 (4370), 30.58 (14 440)[b]		8.7 (8.5)	1.7 (1.8)	2.45	*f*
[Pd{PhTe(CH$_2$)$_3$TePh}Cl$_2$]	yellow	25.38 (13 520)	305, 290	28.6 (28.8)	2.5 (2.5)		
[Pd{PhTe(CH$_2$)$_3$TePh}Br$_2$]	orange	24.57 (10 040)	220	25.1 (25.0)	2.2 (2.1)		
[Pd{PhTe(CH$_2$)$_3$TePh}I$_2$]	red	21.46 (3380), 28.17 (sh) (9720)		22.1 (22.0)	2.0 (2.1)		
[Pt{MeTe(CH$_2$)$_3$TeMe}Cl$_2$]	pale yellow	26.67 (sh) (424), 30.86 (sh) (1680)[b]	301, 287	10.1 (9.9)	2.0 (2.0)	2.22 (32)	2.19 (*f*)
[Pt{MeTe(CH$_2$)$_3$TeMe}Br$_2$]	yellow	25.64 (450), 30.12 (sh) (2680)[b]	218	8.8 (9.0)	1.8 (1.9)	2.32 (34)	2.30 (32)
[Pt{MeTe(CH$_2$)$_3$TeMe}I$_2$]	orange	26.46 (2970), 30.77 (sh) (4170)[b]		7.7 (7.6)	1.5 (1.6)	2.42 (33)	*f*
[Pt{PhTe(CH$_2$)$_3$TePh}Cl$_2$]	pale yellow	24.39 (sh) (300), 29.41 (sh) (1520), 34.48 (5270)	305, 290	25.1 (24.9)	2.2 (2.3)		
[Pt{PhTe(CH$_2$)$_3$TePh}Br$_2$]	yellow	25.64 (sh) (400), 33.33 (sh) (4430)	224	22.3 (22.4)	2.0 (2.0)		
[Pt{PhTe(CH$_2$)$_3$TePh}I$_2$]	orange	25.97 (4160)		20.0 (20.1)	1.8 (1.9)		

[a] In dimethyl sulfoxide solution. [b] In *N,N*-dimethylformamide solution. [c] Nujol mulls. [d] Calculated values in parentheses. [e] Methyl resonances only, with $^3J(^{195}Pt-^1H)$ (in Hz) in parentheses. [f] Resonance of minor invertomer not clearly identified.

Figure 1. Structures of *meso* and *dl* invertomers.

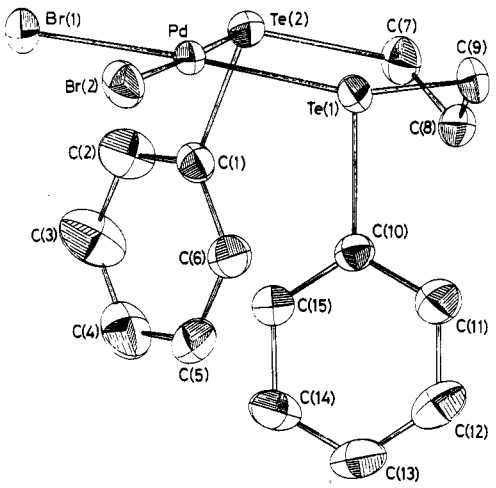

Figure 2. View of discrete molecule showing the atom-numbering scheme. Thermal ellipsoids were drawn with 40% probability boundary surfaces and with hydrogen atoms omitted for clarity.

in *trans*-PdBr$_2$(C$_9$H$_7$NS)$_2$.[12] The ligand forms a six-membered chelate ring in which five atoms are approximately coplanar with the sixth (C(8)) out of the plane by 0.73 Å—the "sofa" conformation. The two phenyl rings lie on the same side of the chelate ring (and on the same side as C(8)) and this gives rise to the syn conformation (*meso* invertomer). Although this chelating ditellurium ligand is unique, five-membered rings with Pd and S_2 ligands[13] and Pt with S_2[14,15] and Se_2[5,16] ligands are known and give rise to in some cases the syn (*meso*) conformation and in other cases the anti (*dl*) conformation in the solid state.

NMR Studies. Little data are available on pyramidal inversion in coordinated telluroethers, but from studies on *trans*-[M-

Table II. Bond Distances (Å) and Angles (deg) for [Pd{PhTe(CH$_2$)$_3$TePh}Br$_2$]

Pd-Br(1)	2.480 (1)	Te(1)-C(9)	2.147 (4)
Pd-Br(2)	2.480 (1)	Te(1)-C(10)	2.129 (4)
Pd-Te(1)	2.528 (1)	Te(2)-C(1)	2.126 (4)
Pd-Te(2)	2.525 (1)	Te(2)-C(7)	2.153 (5)
C(7)-C(8)	1.500 (6)	Br(1)···Br(2)	3.621 (2)
C(8)-C(9)	1.528 (6)	Br(1)···Te(2)	3.313 (2)
C-H(fixed)	0.95	Br(2)···Te(1)	3.348 (2)
		Te(1)···Te(2)	3.855 (2)
Br(1)-Pd-Br(2)	93.8 (1)	Te(2)-C(7)-C(8)	121.0 (3)
Br(1)-Pd-Te(2)	82.9 (1)	C(7)-C(8)-C(9)	114.7 (4)
Br(2)-Pd-Te(1)	83.9 (1)	C(8)-C(9)-Te(1)	117.5 (3)
Te(1)-Pd-Te(2)	99.4 (1)		
Pd-Te(1)-C(9)	111.0 (1)	Pd-Te(2)-C(1)	100.5 (1)
Pd-Te(1)-C(10)	99.9 (1)	Pd-Te(2)-C(7)	113.4 (1)
C(9)-Te(1)-C(10)	93.6 (2)	C(1)-Te(2)-C(7)	95.2 (2)

(ER$_2$)$_2$X$_2$][17] it appears that the barriers to inversion are in the order S < Se < Te. The δ(Me) resonances in the proton NMR spectra of [Pd{MeTe(CH$_2$)$_3$TeMe}X$_2$] showed no evidence of broadening or coalescence over the temperature range 298–353 K in DMSO solution, although the solutions darkened probably due to some decomposition. It seems likely that the barrier energies to inversion in these compounds are too high to study by VTNMR methods, and NMR studies were limited to establishing trends in the static data (at 298 K) and to a comparison with data on the diselenoether analogues. The ^{1}H NMR data are given in Table I, the ^{125}Te{^{1}H} and ^{77}Se{^{1}H} data in Table III, and the ^{195}Pt{^{1}H} in Table IV. It is convenient to discuss each nucleus in turn.

^{1}H NMR. The [M{MeTe(CH$_2$)$_3$TeMe}X$_2$] (X = Cl or Br) complexes show two methyl resonances, in the case of M = Pt with satellites due to coupling to ^{195}Pt. The major resonance to high frequency is identified as that due to the *meso* invertomer by comparison with the data on dithio-[18] and diselenoether[4] analogues. The structure of the [Pd{PhTe(CH$_2$)$_3$TePh}Br$_2$] also supports the isomer identification. Correlation of solid structure with the major solution form is generally open to considerable doubt and in some areas, e.g. isopolyanions, is notorious for the erroneous conclusions drawn in the older literature. However in cases like the present involving two diastereoisomers, it appears a more reasonable approach. Three X-ray studies—[Re(CO)$_3$I{*meso*-MeSe(CH$_2$)$_2$SeMe}][19] and [PtMe$_3$X{*meso*-MeSeCH=CHSeMe}] (X = Cl or I)[16]—have found that the

(11) Wieghardt, K.; Küppers, H.-J.; Raabe, E.; Krüger, C. *Angew. Chem., Int. Ed. Engl.* **1986**, *25*, 1101.
(12) Giordano, T. J.; Butler, W. M.; Rasmussen, P. G. *Inorg. Chem.* **1978**, *17*, 1917.
(13) Pin-Xi, S.; Xinkan, Y.; Yi-Xing, G. *Acta Chim. Sin.* **1984**, *42*, 20.
(14) Hunter, W. N.; Muir, K. W.; Sharp, D. W. A. *Acta Crystallogr.* **1986**, *42C*, 961.
(15) Cano, O.; Leal, J.; Quintana, P.; Torrens, H. *Inorg. Chim. Acta* **1984**, *89*, L9.
(16) Abel, E. W.; Bhargava, S. K.; Orrell, K. G.; Platt, A. W. G.; Sik, V.; Cameron, T. S. *J. Chem. Soc., Dalton Trans.* **1985**, 345.
(17) Cross, R. J.; Green, T. H.; Keat, R. *J. Chem. Soc., Dalton Trans.* **1976**, 1150. Cross, R. J.; Green, T. H.; Keat, R.; Paterson, J. *J. Chem. Soc., Dalton Trans.* **1976**, 1486.
(18) Abel, E. W.; Bhargava, S. K.; Kite, K.; Orrell, K. G.; Sik, V.; Williams, B. L. *Polyhedron* **1982**, *1*, 289.
(19) Abel, E. W.; Bhargava, S. K.; Bhatti, M. M.; Kite, K.; Mazid, M. A.; Orrell, K. G.; Sik, V.; Williams, B. L.; Hursthouse, M. B.; Malik, K. M. A. *J. Chem. Soc., Dalton Trans.* **1982**, 2065.

Table III. $^{125}Te\{^1H\}$ and $^{77}Se\{^1H\}$ NMR Chemical Shift Data[a,b]

complex	*meso*	*dl*	*meso*:*dl*[c]	Δ(Te:Se)[d]
$[Pd\{MeTe(CH_2)_3TeMe\}Cl_2]$[e]	421	340	~10:1	319, 238
$[Pd\{MeTe(CH_2)_3TeMe\}Br_2]$[e]	399	319	~10:1	297, 217
$[Pd\{MeTe(CH_2)_3TeMe\}I_2]$[e]	320	261	~15:1	218, 159
$[Pd\{PhTe(CH_2)_3TePh\}Cl_2]$[f]	588	556	~10:1	132, 100
$[Pd\{PhTe(CH_2)_3TePh\}Br_2]$[f]	564	531	~10:1	108, 75
$[Pd\{PhTe(CH_2)_3TePh\}I_2]$[f]	512	477	~15:1	56, 21
$[Pt\{MeTe(CH_2)_3TeMe\}Cl_2]$[e]	376 (1140)	313 (820)	~10:1	274, 211
$[Pt\{MeTe(CH_2)_3TeMe\}Br_2]$[e]	361 (826)	307 (680)	~20:1	257, 204
$[Pt\{MeTe(CH_2)_3TeMe\}I_2]$[e]	314 (257)	275 (113)	~20:1	212, 173
$[Pt\{PhTe(CH_2)_3TePh\}Cl_2]$[e]	566 (1600)	540 (1200)	~5:1	110, 84
$[Pt\{PhTe(CH_2)_3TePh\}Br_2]$[e]	559 (1240)	529 (970)	~10:1	103, 73
$[Pt\{PhTe(CH_2)_3TePh\}I_2]$[f]	525 (615)	499 (415)	~20:1	69, 43
$[Pt\{MeSe(CH_2)_3SeMe\}Cl_2]$[f]	178 (500)	163 (518)	~3:1	112, 97
$[Pt\{MeSe(CH_2)_3SeMe\}Br_2]$[f]	171.5 (441)	163 (400)	~3:1	105, 97
$[Pt\{MeSe(CH_2)_3SeMe\}I_2]$[f]	163 (230)	152 (180)	~3:1	97, 86
$[Pt\{PhSe(CH_2)_3SePh\}Cl_2]$[e]	314 (625)	309 (576)	~3:1	33, 28
$[Pt\{PhSe(CH_2)_3SePh\}Br_2]$[e]	307 (300)	303 (480)	~2:1	26, 22
$[Pt\{PhSe(CH_2)_3SePh\}I_2]$[e]	303.5 (300)	301.5 (295)	~2:1	22, 20

[a] Relative to external neat $TeMe_2$ or $SeMe_2$ ($\delta = 0$). [b] $^1J(^{195}Pt-^{125}Te)$ or $^1J(^{195}Pt-^{77}Se)$ coupling constants in parentheses (Hz). [c] Approximate isomer population. [d] Coordination shift (δ(complex) − δ(free ligand)). Free ligand shifts: $MeTe(CH_2)_3TeMe$ in DMF = 102 ppm, $PhTe(CH_2)_3TePh$ in DMSO = 456 ppm, $PhSe(CH_2)_3SePh$ in DMF = 281 ppm, and $MeSe(CH_2)_3SeMe$ in DMSO = 64 ppm. [e] *N,N*-Dimethylformamide solution. [f] Dimethyl sulfoxide solution.

Table IV. $^{195}Pt\{^1H\}$ NMR Chemical Shift Data[a]

complex	*meso*	*dl*
$[Pt\{MeS(CH_2)_3SMe\}Cl_2]$[b]	−3570	−3538
$[Pt\{MeS(CH_2)_3SMe\}Br_2]$[b]	−3922	−3893
$[Pt\{MeS(CH_2)_3SMe\}I_2]$	−4706	−4680
$[Pt\{PhS(CH_2)_3SPh\}Cl_2]$[b]	−3584	−3544
$[Pt\{PhS(CH_2)_3SPh\}Br_2]$	−3976	−3948
$[Pt\{PhS(CH_2)_3SPh\}I_2]$	−4805	
$[Pt\{MeSe(CH_2)_3SeMe\}Cl_2]$[c]	−3715	−3662
$[Pt\{MeSe(CH_2)_3SeMe\}Br_2]$[c]	−4165	−4121
$[Pt\{MeSe(CH_2)_3SeMe\}I_2]$	−4933	−4901
$[Pt\{PhSe(CH_2)_3SePh\}Cl_2]$	−3720	−3719
$[Pt\{PhSe(CH_2)_3SePh\}Br_2]$	−4175	−4170
$[Pt\{PhSe(CH_2)_3SePh\}I_2]$	−5056	−5030
$[Pt\{MeTe(CH_2)_3TeMe\}Cl_2]$	−4434	−4379
$[Pt\{MeTe(CH_2)_3TeMe\}Br_2]$	−4846	−4809
$[Pt\{MeTe(CH_2)_3TeMe\}I_2]$	−5639	−5622
$[Pt\{PhTe(CH_2)_3TePh\}Cl_2]$	−4406	−4387
$[Pt\{PhTe(CH_2)_3TePh\}Br_2]$	−4845	−4825
$[Pt\{PhTe(CH_2)_3TePh\}I_2]$[b]	−5696	−5672

[a] δ relative to external 1 mol dm^{-3} $[PtCl_6]^{2-}$ in H_2O ($\delta = 0$) in *N,N*-dimethylformamide solution except compounds denoted with footnote *b*. [b] Dimethyl sulfoxide solution. [c] Values reported in ref 4 are erroneous.

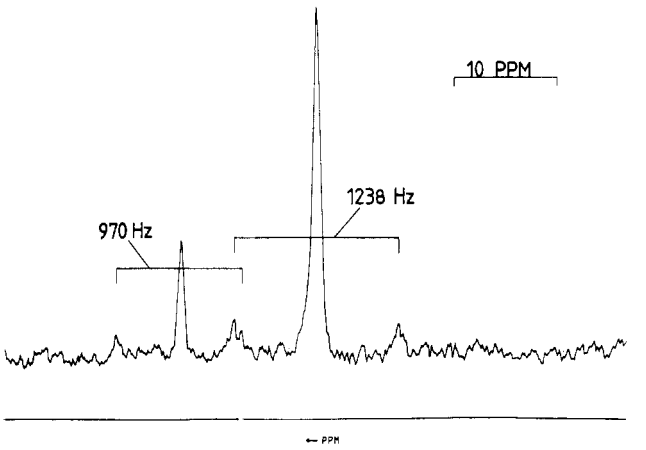

Figure 3. $^{195}Pt\{^1H\}$ NMR spectrum of $[Pt\{PhTe(CH_2)_3TePh\}Br_2]$ in DMF (40×10^3 transients; 298 K).

geometry in the crystal corresponds to that of the major invertomer in solution. For $[M\{MeTe(CH_2)_3TeMe\}I_2]$ only one resonance in each was certainly identified, which is assigned to the *meso* invertomer. The ^{195}Pt and ^{125}Te NMR data below show that the abundance of the second isomer is very low, and in the proton spectra it could not be clearly identified since ligand backbone signals appear in the same region. The δ(Me) resonances show the usual high frequency shift with trans ligand,[4] Cl < Br < I, and for the platinum complexes $^3J(^{195}Pt-^1H)$ is ca. 33 Hz (Table I).

$^{195}Pt\{^1H\}$ NMR. The platinum NMR spectra reveal two resonances with ^{125}Te satellites, of very disparate intensity for each complex. A typical example is shown in Figure 3. The more intense resonance (*meso* invertomer) has the more negative chemical shift, the differences between the two invertomers ranging from 20 to 55 ppm. There is very little literature data on ^{195}Pt spectra of tellurium complexes.[20,21] The data in Table IV show that there is a low-frequency shift with halogen, Cl > Br > I, which is also observed with dithio- and diselenoether complexes. Within each type, replacement of Cl by Br results in a shielding of ca. 400 ppm, and replacement of Br by I results in a further shielding of ca. 800 ppm. Changes in the terminal groups on the bidentate ligand (Me for Ph) have only small effects on δ(Pt), but changing the donor from S to Se to Te produces systematic low-frequency shifts. For constant X, replacement of dithio- by diseleno-ether produces a shift of *ca* −200 ppm, and diseleno- by ditelluro-ether has a larger effect *ca* −700 ppm. The effect on the δ(Pt) as group 16 is descended is consistent with the order of shifts with halide Cl > Br > I.

$^{125}Te\{^1H\}$ NMR. Tellurium-125 is a nucleus of only moderate NMR sensitivity ($I = {}^1/_2$, 7%, Dp = 2.21×10^{-3}),[20] and this combined with the poor solubility of the complexes resulted in long accumulations being required (typically $(250–350) \times 10^3$ transients). A typical spectrum is shown in Figure 4. Even then the low abundance of the minor invertomer (*dl*) made it difficult to measure the $^1J(^{195}Pt-^{125}Te)$ couplings accurately for this form, and the data in Table III should be viewed in that light. The ^{125}Te chemical shifts of the free ligands are known to be temperature, concentration, and solvent dependent.[3,22] For the complexes the ^{125}Te chemical shift varied by a few ppm (<10) between DMF and DMSO solutions, but poor solubility prevented studies in other solvents.

Coordination of the ditelluroethers to a metal results in a high-frequency shift of the tellurium resonance, again with trans halogen dependence Cl > Br > I and with the palladium complexes

(20) Mason, J., Ed. *Multinuclear NMR*; Plenum: New York, 1987.
(21) Pregosin, P. S. *Coord. Chem. Rev.* **1982**, *44*, 247.
(22) Luthra, N. P.; Odom, J. D. In *The Chemistry of Organic Selenium and Tellurium Compounds*; Patai, S., Rappoport, Z., Eds.; Wiley: New York, 1986, Vol. 1, pp 189–241.

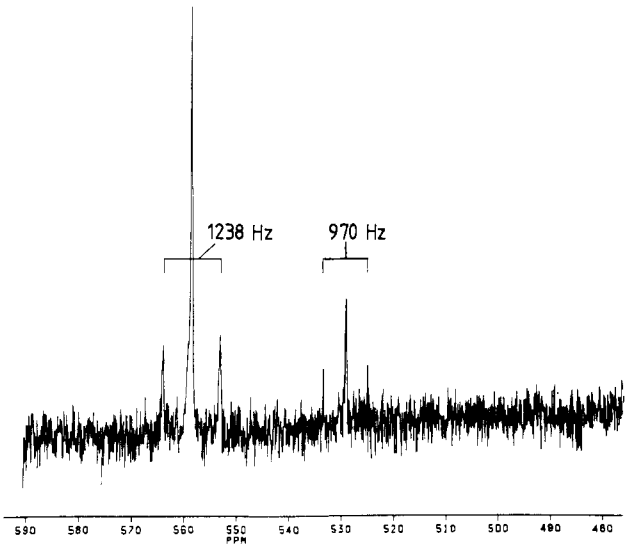

Figure 4. $^{125}Te\{^{1}H\}$ NMR spectrum of $[Pt\{PhTe(CH_2)_3TePh\}Br_2]$ in DMF (350×10^3 transients; 298 K).

having larger shifts than the platinum analogues. The different invertomers have δ(Te) values that differ by ≤80 ppm, and the ^{125}Te spectra are particularly convenient for studying the invertomers (cf. ref 4, 23). The *meso* invertomer has the higher frequency resonance. Comparison of the coordination shifts (Table III) reveals these to be greater for the $MeTe(CH_2)_3TeMe$ complexes than for those of $PhTe(CH_2)_3TePh$. These trends are paralleled by the corresponding ^{77}Se data on $RSe(CH_2)_3SeR$ (Table III), although in five-membered chelate rings ($RSe(CH_2)_2SeR$ complexes) the *dl* isomer has the more positive shift and the halogen dependence is reversed (Cl < Br < I).[4] As yet no data for five-membered-ring ditelluroether complexes are available to complete the pattern, and in its absence the existence of a characteristic *ring contribution* to δ(Te), which is present in ^{77}Se and ^{31}P data on diselenoether and diphosphine complexes,[4,24] is unclear.

Table III also lists ^{77}Se data on complexes of $MeSe(CH_2)_3SeMe$ and $PhSe(CH_2)_3SePh$. The complexes of the latter decompose immediately in DMSO with liberation of free ligand,[4] but in DMF solution with added $[Cr(acac)_3]$ as a relaxation agent, data could be acquired in about 4 h (typically 40×10^3 transients), during which about 10–20% decomposition occured.

The $^1J(^{195}Pt\text{-}^{125}Te)$ coupling constants are listed in Table III. The signs are undetermined, but by comparison with $[Pt(Me_2Te)X_3]^-$[25] are probably negative. The magnitudes of $^1J(^{195}Pt\text{–}^{125}Te)$ decreased in the order Cl > Br > I, reflecting the usual dependence upon the trans influence of the trans halide,[21] as observed in $^1J(^{195}Pt\text{–}^{77}Se)$ and $^1J(^{195}Pt\text{–}^{31}P)$ in selenoether and tertiary phosphine complexes.[4,21,26,27] The effect of invertomer is notable with the *meso* isomer having the larger value of ^1J, although as pointed out in connection with the generally similar trends in $^1J(^{195}Pt\text{–}^{77}Se)$, the coupling constant is likely to be very sensitive to the orientation of the free lone pair and is probably not a reliable indicator of bond strength differences in the two invertomers. Few values for $^1J(^{195}Pt\text{–}^{125}Te)$ are available for comparison, but we note values of 900 Hz for *cis*-$[Pt\{Te(CH_2CH_2Ph)_2\}_2Cl_2]$,[28] −1553 Hz for $[Pt(Me_2Te)Cl_3]^-$, −1092 Hz for $[Pt(Me_2Te)Br_3]^-$, and −400 Hz for $[Pt(Me_2Te)I_3]^-$.[25]

It is now possible to compare corresponding dithioether, diselenoether, and ditelluroether complexes. Particularly notable is the invertomer ratio. In five-membered chelate ring complexes, $[M(L\text{-}L)X_2]$ (L-L = $RECH_2CH_2ER$ and E = S or Se), the *dl* invertomer is most abundant,[4] although the *dl*:*meso* ratio is not particularly disparate (≤4:1). For the six-membered rings, data appear to be available only for one dithioether $[Pt\{MeS(CH_2)_3SMe\}Cl_2]$,[18] where the invertomers are of approximately equal abundance. For $[Pt\{RSe(CH_2)_3SeR\}X_2]$ (Table III) the *meso* form predominates, and in complexes of the two ditelluroethers the *meso*:*dl* ratio ranges from 5:1 to ca. 20:1. In complexes of six-coordinate platinum, e.g. $[PtMe_3X(L\text{-}L)]$ the *meso*:*dl* ratios are influenced by steric interactions with the axial ligands,[16] but this effect is necessarily absent in planar complexes. In the latter it seems likely that the major influence is strain within the ring as the ring size and donor atoms change, although the dependence of the *meso*:*dl* ratio upon the trans halide shows that electronic effects also influence the invertomer population.

McFarlane[29] showed in an early study that for comparable organocompounds the δ(Te) and δ(Se) resonances had an effectively constant ratio of ca. 1.8 (although theoretical explanation of the value has proved elusive[20]). The present work allows similar comparison in Se and Te donor ligand *complexes*. We find that comparison of the data in Table III for fixed M, X, and invertomer, shows the δ(Te):δ(Se) ratio ranges from 2.11 to 1.66 with an average of 1.8 (6). In view of the very different electronic environment in the complexes and the conformational limitations imposed by chelation, the appearance of the same approximate ratio is remarkable and suggests that it may be similarly useful predictively.

Attempted Oxidation. We have described elsewhere the halogen (Cl_2 or Br_2) oxidation of platinum(II) dithioether[30] and diselenoether[5] complexes to stable Pt(IV) analogues $[Pt(L\text{-}L)X_4]$. In contrast, the Pd(II) complexes do not oxidize and the only examples of Pd(IV) complexes with neutral group 16 donor ligands are the unstable $[Pd(Me_2E)X_5]^-$ ions (E = S or Se; X = Cl or Br).[5,31] However the palladium(II) or platinum(II) ditelluroether complexes were recovered unchanged after stirring with stoichiometric amounts of halogen in CCl_4. Under more forcing conditions, i.e. a large excess of chlorine for several hours, $[Pt\{PhTe(CH_2)_3TePh\}Cl_2]$ was converted into a darker material of variable composition. The far-IR spectra of these products showed ν(Pt–Cl) stretches of the starting material and a new band at ca. 340 cm^{-1} which suggests the presence of $[PtCl_6]^{2-}$.[32] Removal of the CCl_4 from one solution and dissolution of the product in DMF gave an orange solution with weak $\delta(^{125}Te)$ NMR resonances of the Pt(II) starting material and a strong resonance at 970 ppm. The white $PhCl_2Te(CH_2)_3TePhCl_2$ (from the ligand + Cl_2) had $\delta(^{125}Te)$ = 965 ppm in DMF, which in view of the concentration sensitivity of organotellurium chemical shifts may be taken as good agreement. Hence we conclude that stable Pt(IV) complexes are not formed; instead, excess halogen decomposes the complexes with oxidation of the ligand and generation of $[PtCl_6]^{2-}$. Attempts to prepare iridium(IV) ditelluroethers have also failed.[33]

Conclusion

The synthesis, properties and structures of the first examples of complexes of chelating ditelluroethers have been described. Detailed multinuclear NMR studies have revealed systematic changes in $\delta(^{125}Te)$ and $\delta(^{195}Pt)$ with diastereoisomer, trans ligand, and metal center. Close parallels between corresponding selenoether and telluroether complexes have been observed.

(23) Gulliver, D. J.; Hope, E. G.; Levason, W.; Murray, S. G.; Marshall, G. L. *J. Chem. Soc., Dalton Trans.* **1985**, 2185.
(24) Garrou, P. E. *Chem. Rev.* **1981**, *81*, 229.
(25) Goggin, P. L.; Goodfellow, R. J.; Haddock, S. R. *J. Chem. Soc., Chem. Commun.* **1975**, 176.
(26) Abel, E. W.; Orrell, K. G.; Platt, A. W. G. *J. Chem. Soc., Dalton Trans.* **1983**, 2545.
(27) Pregosin, P. S. In *Phosphorus-31 NMR Spectroscopy in Stereochemical Analysis*; Verkade, J. G., Quin, L. D., Eds.; VCH Publishers: Deerfield Beach, FL, 1987; Chapter 14.
(28) Gysling, H. J.; Zumbulyadis, N.; Robertson, J. A. *J. Organomet. Chem.* **1981**, *209*, C41.
(29) McFarlane, H. C. E.; McFarlane, W. *J. Chem. Soc., Dalton Trans.* **1973**, 2416.
(30) Gulliver, D. J.; Levason, W.; Smith, K. G.; Selwood, M. J.; Murray, S. G. *J. Chem. Soc., Dalton Trans.* **1980**, 1872.
(31) Gulliver, D. J.; Levason, W. *J. Chem. Soc., Dalton Trans.* **1982**, 1895.
(32) Hiraishi, J.; Nakagawa, I.; Shimanouchi, T. *Spectrochim. Acta* **1964**, *20*, 819.
(33) Cipriano, R. A.; Levason, W.; Pletcher, D.; Powell, N. A.; Webster, M. *J. Chem. Soc., Dalton Trans.* **1987**, 1901.

Table V. Atomic Coordinates for [Pd{PhTe(CH$_2$)$_3$TePh}Br$_2$]

	x	*y*	*z*	*U*,[a] Å^2
Pd	0.33486 (4)	0.36572 (3)	0.83706 (4)	32.2 (2)
Te(1)	0.56582 (4)	0.27446 (3)	0.95831 (3)	34.7 (2)
Te(2)	0.44843 (4)	0.43732 (3)	0.68576 (3)	35.5 (2)
Br(1)	0.09613 (6)	0.44383 (5)	0.71578 (6)	49.7 (2)
Br(2)	0.20883 (6)	0.29963 (5)	0.97949 (6)	49.1 (2)
C(1)	0.2734 (6)	0.2843 (4)	0.4776 (5)	37 (2)
C(2)	0.1744 (8)	0.3237 (5)	0.3775 (6)	62 (2)
C(3)	0.0615 (9)	0.2286 (7)	0.2402 (6)	79 (3)
C(4)	0.0456 (8)	0.0954 (7)	0.2034 (6)	70 (3)
C(5)	0.1421 (8)	0.0537 (6)	0.3026 (7)	70 (2)
C(6)	0.2582 (7)	0.1482 (5)	0.4424 (6)	59 (2)
C(7)	0.6687 (6)	0.3786 (5)	0.6923 (5)	46 (2)
C(8)	0.7081 (6)	0.2671 (5)	0.7375 (5)	43 (2)
C(9)	0.7635 (6)	0.3002 (5)	0.8965 (5)	43 (2)
C(10)	0.4503 (6)	0.0654 (4)	0.8176 (5)	37 (2)
C(11)	0.5453 (7)	−0.0198 (5)	0.8429 (6)	56 (2)
C(12)	0.4714 (9)	−0.1572 (5)	0.7568 (7)	63 (3)
C(13)	0.3069 (8)	−0.2093 (5)	0.6494 (6)	60 (2)
C(14)	0.2122 (8)	−0.1252 (5)	0.6253 (7)	69 (2)
C(15)	0.2847 (7)	0.0139 (5)	0.7105 (6)	52 (2)

[a] Equivalent isotropic temperature factor from anisotropic atom (× 10^3). *U* = one-third of the trace of the orthogonalized *U*.

Experimental Section

Physical data were recorded as described previously.[3-5,34,35] ^{125}Te{^{1}H} data were recorded on a Bruker AM360 instrument at 113.6 MHz on saturated solutions in DMSO or DMF containing 5% deuteriated solvent to provide the lock and are referenced to neat external Me_2Te.[3] ^{77}Se{^{1}H} spectra were recorded as described,[4] except those for PhSe(CH$_2$)$_3$SePh complexes, which were run in freshly prepared DMF solutions containing ca. 5 mg of [Cr(acac)$_3$] with no relaxation delay. The ligands[3] and dithioether[30] and diselenoether[4] complexes were made by literature methods. Representative preparations for two telluroether complexes are described.

Dichloro[1,3-bis(phenyltelluro)propane]platinum(II). The ligand (0.113 g, 0.25 mmol) was added to a rapidly stirred solution of [Pt(MeCN)$_2$Cl$_2$] (0.087 g, 0.25 mmol) in dichloromethane (25 cm^3) and stirred for 3 h. The precipitate was filtered off, washed with diethyl ether and dried in vacuo. Yield: 0.172 g, 96%

Dibromo(2,6-ditelluraheptane)platinum(II). An excess of sodium bromide dissolved in water (5 cm^3) was added to [Pt(MeCN)$_2$Cl$_2$] (0.087 g, 0.25 mmol) in acetontrile (40 cm^3). The mixture was refluxed for 4 h and then allowed to cool. The ligand (0.082 g, 0.25 mmol) was added dropwise with vigorous stirring. After 3 h the precipitate was filtered off, washed with water, acetonitrile, and diethyl ether, and dried. Yield: 0.158 g, 92%

X-ray Data and Structure Solution. Orange air-stable rhomb-shaped crystals were grown from diethyl ether–acetonitrile solutions. Preliminary photographic X-ray examination established the crystal system and approximate cell dimensions. Accurate cell dimensions were obtained from 25 carefully centered reflections on an Enraf-Nonius CAD-4 diffractometer equipped with Mo Kα radiation.

The crystals are triclinic, a = 8.968 (1) Å, b = 10.978 (1) Å, c = 11.070 (2) Å, α = 108.16 (1)°, β = 113.15 (1)°, γ = 98.95 (1)°, V = 902.65 Å^3, and mol wt of 717.7 for $C_{15}H_{16}Br_2PdTe_2$. D_{meas} = 2.60 (4) (flotation), D_{calc} = 2.640 g cm^{-3} for Z = 2, space group $P\bar{1}$ (from the analysis), $F(000)$ = 652, and μ(Mo Kα) = 85.1 cm^{-1}.

A crystal at room-temperature (0.3 × 0.07 × 0.2 mm) was mounted in a thin-wall glass capillary. Data were collected with Mo Kα radiation (λ = 0.710 69 Å) and graphite monochromator. In total, 3394 reflections were measured (1.5° < θ < 25°; h (0 to 10), k (−13 to +13), l (−13 to +13)), and after averaging (R_{int} = 0.012), there remained 3172 unique reflections. No decay was observed in the measured check reflections and an empirical ψ-scan absorption correction was applied to the data (transmission: maximum, 100.0%; minimum 60.0%) together with the usual *Lp* factor. Omitting observations with $F < 3\sigma(F)$ (625) left 2547 used in the analysis.

The *E* statistics favored the centrosymmetric space group $P\bar{1}$, and the structure was solved by the direct methods strategy (EEES) available in SHELX.[35] The *E* maps all contained multiple images of the $PdBr_2Te_2$ residue, and the correct solution was established by repeated structure factor and electron density calculations. Hydrogen atoms were added in calculated positions (d(C–H) = 0.95 Å) and two reflections (010; 021) thought to be suffering from extinction were removed. Full-matrix least-squares refinement minimizing $\Sigma w(|F_o| - |F_c|)^2$ converged to R = 0.023 [R_w = 0.022, 182 parameters, 2545 reflections, anisotropic (Pd, Te, Br, C) thermal parameters, $w = 1/(\sigma^2(F) + 0.00003F^2)$, maximum shift/error = 0.1]. The final difference electron-density synthesis showed all features in the range +0.52 to −0.56 e Å^{-3}. Scattering factors for neutral atoms and anomalous dispersion corrections were taken from SHELX (Br, C, H) and ref 36 (Pd, Te), and all calculations were performed on an IBM3090 computer using the programs SHELX,[35] ORTEP,[37] and XANADU.[38]

The non-hydrogen atomic positions are given in Table V, and other structural parameters are available as supplementary material.

Acknowledgment. We thank the SERC for support (T.K.) and Dr. M. B. Hursthouse for the X-ray data collection on the Queen Mary College, London/SERC diffractometer.

Registry No. *meso*-[Pd(MeTe(CH$_2$)$_3$TeMe)Cl$_2$], 118376-91-3; *meso*-[Pd(MeTe(CH$_2$)$_3$TeMe)Br$_2$], 118376-92-4; *meso*-[Pd(MeTe(CH$_2$)$_3$TeMe)I$_2$], 118376-93-5; *meso*-[Pd(PhTe(CH$_2$)$_3$TePh)Cl$_2$], 118376-94-6; *meso*-[Pd(PhTe(CH$_2$)$_3$TePh)Br$_2$], 118376-95-7; *meso*-[Pd(PhTe(CH$_2$)$_3$TePh)I$_2$], 118376-96-8; *meso*-[Pt(MeTe(CH$_2$)$_3$TeMe)Cl$_2$], 118376-97-9; *meso*-[Pt(MeTe(CH$_2$)$_3$TeMe)Br$_2$], 118376-98-0; *meso*-[Pt(MeTe(CH$_2$)$_3$TeMe)I$_2$], 118376-99-1; *meso*-[Pt(PhTe(CH$_2$)$_3$TePh)Cl$_2$], 118377-00-7; *meso*-[Pt(PhTe(CH$_2$)$_3$TePh)Br$_2$], 118377-01-8; *meso*-[Pt(PhTe(CH$_2$)$_3$TePh)I$_2$], 118377-02-9; [Pd(MeCN)$_2$Cl$_2$], 14592-56-4; [Pd(MeCN)$_2$Br$_2$], 53623-19-1; [Pd(MeCN)$_2$I$_2$], 118377-03-0; [Pt(MeCN)$_2$Cl$_2$], 13869-38-0; [Pt(MeCN)$_2$Br$_2$], 13869-36-8; [Pt(MeCN)$_2$I$_2$], 118377-04-1; *dl*-[Pd(MeTe(CH$_2$)$_3$TeMe)Cl$_2$], 118455-52-0; *dl*-[Pd(MeTe(CH$_2$)$_3$TeMe)Br$_2$], 118455-53-1; *dl*-[Pd(MeTe(CH$_2$)$_3$TeMe)I$_2$], 118455-54-2; *dl*-[Pd(PhTe(CH$_2$)$_3$TePh)Cl$_2$], 118455-55-3; *dl*-[Pd(PhTe(CH$_2$)$_3$TePh)Br$_2$], 118455-56-4; *dl*-[Pd(PhTe(CH$_2$)$_3$TePh)I$_2$], 118455-57-5; *dl*-[Pt(MeTe(CH$_2$)$_3$TeMe)Cl$_2$], 118455-58-6; *dl*-[Pt(MeTe(CH$_2$)$_3$TeMe)Br$_2$], 118455-59-7; *dl*-[Pt(MeTe(CH$_2$)$_3$TeMe)I$_2$], 118455-60-0; *dl*-[Pt(PhTe(CH$_2$)$_3$TePh)Cl$_2$], 118455-61-1; *dl*-[Pt(PhTe(CH$_2$)$_3$TePh)Br$_2$], 118455-62-2; *dl*-[Pt(PhTe(CH$_2$)$_3$TePh)I$_2$], 118455-63-3; *dl*-[Pt(MeSe(CH$_2$)$_3$SeMe)Cl$_2$], 98931-78-3; *dl*-[Pt(MeSe(CH$_2$)$_3$SeMe)Br$_2$], 98912-51-7; *dl*-[Pt(MeSe(CH$_2$)$_3$SeMe)I$_2$], 98931-79-4; *dl*-[Pt(PhSe(CH$_2$)$_3$SePh)Cl$_2$], 118455-64-4; *dl*-[Pt(PhSe(CH$_2$)$_3$SePh)Br$_2$], 118455-65-5; *dl*-[Pt(PhSe(CH$_2$)$_3$SePh)I$_2$], 118377-05-2; *meso*-[Pt(MeSe(CH$_2$)$_3$SeMe)Cl$_2$], 99397-10-1; *meso*-[Pt(MeSe(CH$_2$)$_3$SeMe)Br$_2$], 99397-09-8; *meso*-[Pt(MeSe(CH$_2$)$_3$SeMe)I$_2$], 99397-08-7; *meso*-[Pt(PhSe(CH$_2$)$_3$SePh)Cl$_2$], 118455-66-6; *meso*-[Pt(PhSe(CH$_2$)$_3$SePh)Br$_2$], 118455-67-7; *meso*-[Pt(PhSe(CH$_2$)$_3$SePh)I$_2$], 118455-68-8; *meso*-[Pt(MeS(CH$_2$)$_3$SMe)Cl$_2$], 84026-96-0; *meso*-[Pt(MeS(CH$_2$)$_3$SMe)Br$_2$], 104975-51-1; *meso*-[Pt(MeS(CH$_2$)$_3$SMe)I$_2$], 118455-69-9; *meso*-[Pt(PhS(CH$_2$)$_3$SPh)Cl$_2$], 118455-70-2; *meso*-[Pt(PhS(CH$_2$)$_3$SPh)Br$_2$], 118455-71-3; *meso*-[Pt(PhS(CH$_2$)$_3$SPh)I$_2$], 118455-72-4; *dl*-[Pt(MeS(CH$_2$)$_3$SMe)Cl$_2$], 71499-16-6; *dl*-[Pt(MeS(CH$_2$)$_3$SMe)Br$_2$], 104975-55-5; *dl*-[Pt(MeS(CH$_2$)$_3$SMe)I$_2$], 118455-73-5; *dl*-[Pt(PhS(CH$_2$)$_3$SPh)Cl$_2$], 118455-74-6; *dl*-[Pt(PhS(CH$_2$)$_3$SPh)Br$_2$], 118455-75-7; ^{125}Te, 14390-73-9; ^{195}Pt, 14191-88-9; ^{77}Se, 14681-72-2; chlorine, 7782-50-5.

Supplementary Material Available: Tables of anisotropic thermal parameters, calculated H atom coordinates, and full bond length and angle data (Tables S-1–S-3) (3 pages); a table of calculated and observed structure factors (Table S-4) (7 pages). Ordering information is given on any current masthead page.

(34) Hope, E. G.; Levason, W.; Powell, N. A. *Inorg. Chim. Acta* **1985**, *115*, 187.
(35) Sheldrick, G. M. "SHELX Program for Crystal Structure Determination"; University Chemical Laboratory: Cambridge, England, 1976.
(36) *International Tables for X-ray Crystallography*; Kynoch: Birmingham, England, 1974; Vol. IV.
(37) Johnson, C. K. *Oak Ridge Natl. Lab., [Rep.] ORNL (U.S.)* **1965**, *ORNL-3794*.
(38) Roberts, P.; Sheldrick, G. M. "XANADU Program for Crystallographic Calculations"; University Chemical Laboratory: Cambridge, England, 1979.